A Normalized Figure of Merit for Capacitive Accelerometer Interface Circuits

Saber Amini, *Member, IEEE,* David Andrew Johns, *Fellow, IEEE*

***Abstract*—This paper proposes a figure of merit for capacitive inertial sensor interface circuits that is a function of the electronic circuitry and not of the mechanical device. The effect of the sensor's sensitivity, sense capacitance and total parasitic capacitance on the overall system's linearity and power consumption is investigated. A literature review of interface circuits is provided showing a tradeoff in linearity and bandwidth when normalized to the specifications of the sensor.**

***Index Terms*—Capacitive sensors, figure of merit, FOM, sensitivity, accelerometers, interface circuits**

I. Introduction

DATA analytics has increasingly been making use of capacitive inertial sensors or accelerometers embedded in mobile and wearable devices [1]. This in turn has led to research efforts into interface circuits that accompany these sensors.

When a system has several competing metrics, often a figure of merit (FOM) is proposed in comparing designs which combines several metrics into a single number. To advance research in the area of interface circuits for inertial sensors, it is important to have a rigorous figure of merit metric that is the property of the circuit, and not of the mechanical device. Finding a fair figure of merit for sensors interfaced with electronics is challenging and an established FOM is yet to be found. The challenge lies in the fact that the specifications of the mechanical sensor will have a great effect on the signal fidelity and power consumption of the overall system.

This concept is demonstrated in Fig. 1 where N_B and N_E represent the mechanical thermal noise and the electronic noise respectively. Depending on the physical parameters of the sensor device, the mechanical and electronic noise change, making the fidelity of the output signal dependent on the sensor. Moreover, the capacitance between the interface circuit and the sensor depends on the physical parameters of the sensor and the implementation of the system, leading to a direct effect on power consumption. This brief investigates these issues and proposes a figure of merit for comparing interface circuits for capacitive accelerometers.

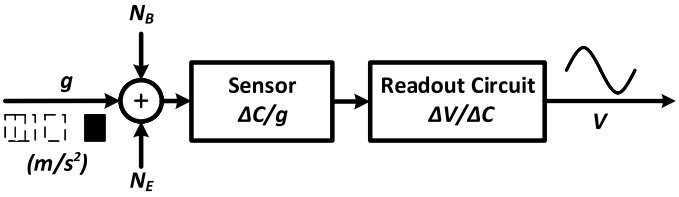

Fig. 1. Block level diagram of a sensor readout system. The gain of the sensor has a major impact on the fidelity of the output signal and can skew comparison between designs.

The brief is organized as follows. Section II details the physical structure of capacitive accelerometers and their dynamics. This information is then used to develop a figure of merit based on the sum of the system's fidelity and bandwidth adjusted to the parameters of the sensor device. Section III then provides a literature review of accelerometer systems comparing them with the proposed FOM. Section IV then makes concluding remarks.

II. Physical Structure of Accelerometers

A differential capacitive accelerometer (Fig. 2(a)-(b)) can be modeled as a set of variable capacitors that change differentially according to

$$C_s^+ = \frac{C_s}{1-\frac{x}{d}} \qquad \text{and} \qquad C_s^- = \frac{C_s}{1+\frac{x}{d}}\ , \tag{1}$$

where C_s is the equivalent sense capacitance of the structure at rest (zero force), d is the nominal distance between the parallel plates (at rest), and x is the displacement under an external force F. The displacement is often modeled as a second order system (Fig. 2(c))

$$x = \frac{a(t)}{s^2+\frac{b}{m}s+\frac{k}{m}}\ , \tag{2}$$

where $a(t)$ is the equivalent acceleration the sensor is undergoing due to to an external force, m is the proof mass in kilograms, k is the spring constant in N/m, and b is the damping coefficient in N/(m/s^2). An alternative form to Eq. (2) is given by

$$x = \frac{a(t)}{s^2+\frac{\omega_n}{Q}s+\omega_n^2}\ , \tag{3}$$

Manuscript received November XX, XXXX. Date of publication July XX, XXXX; date of current version August XX, XXXX. This work was supported in part by the National Sciences and Engineering Research Council of Canada.

The authors are with the Edward S. Rogers Sr. Department of Electrical and Computer Engineering, University of Toronto, Toronto, Ontario Canada (email samini@ieee.org; johns@eecg.utoronto.ca).

Digital Object Identifier XXXXXXXXXXXXXXXXXXXXX

This article has been accepted for publication in a future issue of this journal, but has not been fully edited. Content may change prior to final publication. Citation information: DOI 10.1109/TCSII.2019.2901851, IEEE Transactions on Circuits and Systems II: Express Briefs

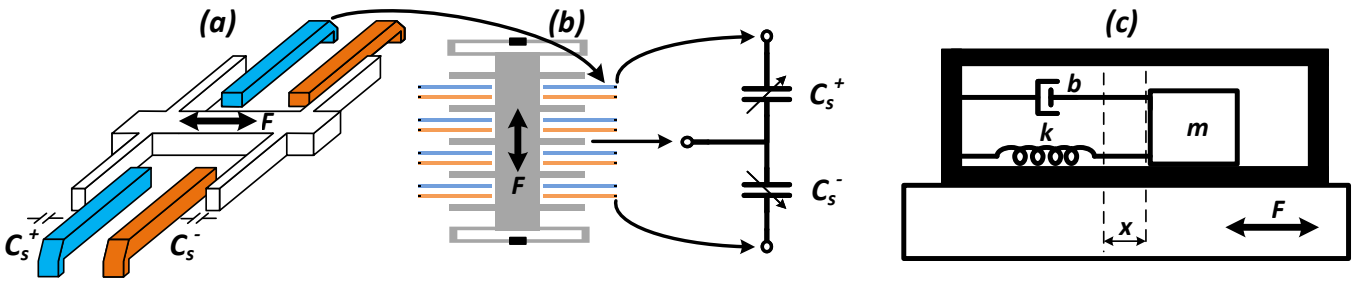

Fig. 2. (a) A surface micromachined accelerometer, (b) simplified electrical model and (c) system level model of the displacement, x.

where ω_n is called the natural frequency and Q is the quality factor. These quantities are related to the physical parameters of the accelerometer according to

$$\omega_n = \sqrt{\frac{k}{m}} \quad \text{and} \quad Q = \frac{\sqrt{km}}{b} \ . \tag{4}$$

For an accelerometer system, it is often desirable to have *critical damping* (where $Q \approx 0.5$), thus avoiding overshoot in the step response as well as ensuring a flat frequency response without peaking. A system design parameter that encompasses the physical properties of the accelerometer is the device sensitivity, S, given by the change in capacitance per unit of earth's gravitational force or fF/g where g=9.8 m/s^2. Sensitivity is related to the physical parameters according to

$$S = \frac{m}{k}\frac{2C_s}{d} \ . \tag{5}$$

In what follows, we will use the mass of the sensor device as a proxy for sensitivity and determine the effect it has on noise and power. The goal is to establish certain factors that normalize the reported SNDR, power and bandwidth and lead to a fair figure of merit.

In regards to noise, the total noise for an accelerometer system is the combination of the mechanical thermal noise (N_B) and the electronic noise (N_E). For analysis, it is convenient to refer these noise sources to the input of the sensor as shown in Fig. 1. Since these noise sources are uncorrelated, we can write the total noise, N_T, as

$$N_T = \sqrt{N_B^2 + N_E^2} \ . \tag{6}$$

The mechanical thermal noise is associated with the random movement of the mass and given by

$$N_B = \sqrt{\frac{4k_BTb}{m^2 \cdot g^2}\frac{w_nQ}{4}} = \frac{\sqrt{k_BTk}}{m \cdot g} \ , \tag{7}$$

where k_B is Boltzmann's constant and T is the temperature in Kelvins.

We would like to determine what effect does the device mass have on the mechanical thermal noise. Assume that the mass of the sensor device is increased by a factor α. To keep the resonant frequency and quality factor of the system the same, according to Eq. (4), this requires both k and b to increase by α. As a result, according to Eq. (7), the increase in mass by a factor α implies that the mechanical noise power of the system, N_B^2, is reduced by α.

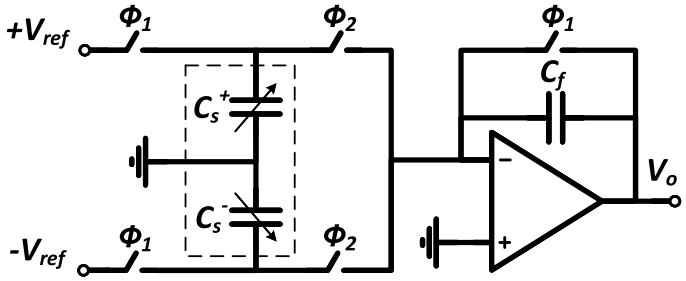

Fig. 3. A simplified switched capacitor interface circuit for differential accelerometers.

Next, we would like to investigate how an increase in mass affects the electronic noise of the system. Based on the typical physical construction of the sensor device as shown in Fig. 2, if the mass increases by α, so must the sense capacitance and conversely the spring constant (to keep the resonant frequency constant). According to Eq. (5), this results in an overall increase in the sensitivity of the sensor by a factor α.

We must now relate this increased sensitivity (due to an increase in mass) to the electronic noise of the interface circuit. Strictly speaking, this would require us to treat each type of interface circuit separately. However, the noise contribution of the various types of interface circuits is within the same order of magnitude [2]. For developing a FOM, we work with the switched capacitor front-end as shown in Fig. 3, as this type of interface circuit is popular and leads to better closed form formulas for the FOM. For simplicity, the effect of parasitic capacitances on noise is ignored in the following analysis as the effect in total noise is minimal [2]. Ignoring parasitic capacitances, the noise of this circuit referred to the input of the sensor is equal to [3]

$$N_E \approx \frac{1}{\sqrt{f_s}}\left[\sqrt{\frac{2k_BT}{2C_s}} + \sqrt{\frac{2k_BT}{C_f}}\frac{C_f}{2C_s}\right]\frac{1}{S \cdot g} \ . \tag{8}$$

Here, f_s is the sampling frequency and C_f is the feedback capacitance. Since the power supply is assumed to be constrained, the best a prudent designer can do is to increase the feedback capacitor, C_f, by the same factor avoiding saturation in the output but reducing the electronic thermal noise according to Eq. (8). In this scenario,

the ratio of the electronic noise power in the new system, $N_{E_1}^2$, over the original system, $N_{E_o}^2$, is given by

$$\frac{N_{E_1}^2}{N_{E_o}^2} = \left[\frac{\sqrt{2\alpha C_s}+\sqrt{\alpha C_f}}{2\alpha C_s}\frac{2C_s}{\sqrt{2C_s}+\sqrt{C_f}}\frac{1}{\alpha}\right]^2 = \frac{1}{\alpha^3} \ . \quad (9)$$

We can therefore state that an increase in sensitivity by a factor α improves the electronic noise power by a factor α^3.

Another parameter that skews comparison of accelerometer systems and directly affects the electronic noise is the dynamic range. Assume that two accelerometer systems with the same sensor and interface circuit are implemented but one accelerometer undergoes acceleration that is λ times higher than the second. For blocks such as filters and analog-to-digital converters, this is akin to having two designs with different power supplies and FOM's generally do not take this into account. This problem, however, is more pronounced for accelerometer systems where dynamic range can be an order of magnitude different between designs and therefore, should be taken into account to achieve a fair comparison. Assuming that the power supply for the two systems is fixed, the increased dynamic range must be compensated by an equivalently larger feedback capacitor. As such, there is an increase in the electronic noise power by

$$\frac{N_{E_1}^2}{N_{E_o}^2} = \left[\frac{\left(\sqrt{2C_s}+\sqrt{\lambda C_f}\right)}{\left(\sqrt{2C_s}+\sqrt{C_f}\right)}\right]^2 \approx \left[\frac{\sqrt{\lambda}+\sqrt{2}}{1+\sqrt{2}}\right]^2 \ , \quad (10)$$

where the approximation has been made by assuming that $C_f \approx C_s$.

One caveat to the above analysis is that it has been developed assuming an open loop system. In a closed loop system, the quality factor and resonant frequency become a strong function of the electronic components [4] and as such, the tradeoffs involving the resonant frequency and quality factor do not apply. In these systems, the mass can be increased without an equivalent increase in damping coefficient and spring constant. This in turn means that an increase in sensitivity by a factor α reduces the mechanical thermal noise power by a factor of α^2. The equations regarding electronic noise, however, hold for closed loop systems as developed above.

In lieu of the above discussion, we introduce a noise factor, $\mathrm{NF_{dB}}$, that takes into account the reduction in the total noise power between two systems where the sensitivity and dynamic range differ by a factor α and λ respectively. Assuming that for power efficiency, $N_{E_o}^2 = N_{B_o}^2$, then the increase/decrease in noise power, referred to the input of the sensor, is given by

$$\mathrm{NF_{dB}} = \frac{N_{T_1}^2}{N_{T_o}^2} = \left[\frac{\sqrt{\lambda}+\sqrt{2}}{\left(1+\sqrt{2}\right)}\right]^2 \frac{1}{2\alpha^3}+\frac{1}{2\alpha^r} \ , \quad (11)$$

where $r = 1$ for open loop system and $r = 2$ for closed loop systems. Using this factor, a normalized SNDR value can be calculated and given by

$$\mathrm{SNDR_{Norm}} = \mathrm{SNDR_{dB}} + \mathrm{NF_{dB}} \ , \quad (12)$$

where $\mathrm{SNDR_{dB}}$ is the reported SNDR value.

Apart from signal fidelity, power and bandwidth play a major role in comparing different systems. It is well accepted that power trades off against bandwidth. However, when a circuit is interfaced with a mechanical sensor, the power consumption is also directly proportional to the total capacitance at the input of the interface circuit [2]. The total input capacitance includes the total sense capacitance of the accelerometer as well as the parasitic capacitance. To produce a factor that takes this into account, we choose a reference sense capacitance, C_{so}, and determine a power factor, $\mathrm{PF_{dB}}$, according to

$$\mathrm{PF_{dB}} = \frac{C_s + C_p}{C_{so}} \ , \quad (13)$$

where C_p is the total parasitic capacitance at the input of the interface circuit. Note that C_{so} value can be chosen arbitrarily. Accordingly, for a fair comparison, we define a normalized bandwidth given by

$$\mathrm{BW_{Norm}} = \mathrm{BW_{dB}} - \mathrm{P_{dB}} + \mathrm{PF_{dB}} \ , \quad (14)$$

where $\mathrm{BW_{dB}}$ and $\mathrm{P_{dB}}$ are the reported bandwidth and power consumption (in dB) respectively. The figure of merit proposed for interface circuits is then the sum of *normalized* SNDR and *normalized* bandwidth (both in dB) and given by

$$\mathrm{FOM} = \mathrm{SNDR_{dB}} + \mathrm{NF_{dB}} + \mathrm{BW_{dB}} - \mathrm{P_{dB}} + \mathrm{PF_{dB}} \quad (15)$$

This FOM indicates that a *higher number* is better and uses a noise factor ($\mathrm{NF_{dB}}$) and a power factor ($\mathrm{PF_{dB}}$) to adjust for different sensor parameters and type of system implementation.

III. Literature Review

A literature review for both open loop and closed loop research based differential capacitive accelerometers is shown in Table I. The reference sensitivity used to normalize the SNDR values is 5.0 fF/g and for acceleration is 1 $\mathrm{g_{rms}}$. Therefore, to get the sensitivity factor, α, the cited sensitivity is divided by the reference sensitivity and λ simply equals the cited acceleration range. The reference sense capacitance, C_{so}, is 350 fF. Unless specifically reported, parasitic capacitance at the interface is estimated to be 100 fF for single chip implementations and 1500 fF for dual chip implementations. If a system reports results in more than one axis or for multiple ranges, the axis or range that provides the best FOM is chosen.

A graphical representation of the figure of merit is shown in Fig. 4 with normalized fidelity on the x-axis and normalized bandwidth on the y-axis. The better performing interface circuits are those that achieve higher signal fidelity relative to the bandwidth and are at the upper right corner of the plot. The dashed lined corresponds to a fixed figure of merit of 120 dB. This plot shows that regardless of the type of sensor used, after normalization for physical parameters, there is a defined tradeoff between SNDR and bandwidth of accelerometer systems.

TABLE I
RESEARCH BASED ACCELEROMETER SYSTEMS SPECIFICATIONS AND PROPOSED FIGURE OF MERIT.

Ref.	Group	Year	Notes[1]	Noise Floor Sensor ($\mu g/\sqrt{Hz}$)	Noise Floor System ($\mu g/\sqrt{Hz}$)	Sensitivity (fF/g)	Range (g_{rms})	BW (Hz)	SNDR (dB)	Power (mW)	FOM (dB)
Closed loop research based systems											
[5]	Sönmez, U.	2014	D	4.6	6	165	15	250	104	16.7	131.7
[6]	Pastre, M.	2009	D	0.8	1.15	393^{E}	11.3	300	98.1	12.0	123.6
[7]	Kulah, H.	2006	D	0.7	10	4900	1.1	500^{E}	100	7.2	118.5
[8]	Amini, B.V.	2006	D	3.87^{C}	4	5000	3.5^{E}	500	91.8^{E}	4.5	109.9
[9]	Condemine	2005	D	2.8^{C}	63.8	348^{E}	10	50	86.9	2.64	111.7
[10]	Petkov, V.	2005	S	41.6^{E}	150	6.6^{E}	4^{E}	100	68.5^{E}	13.0	111.1
[11]	Lemkin, M.	1999	S	83	110	20^{E}	10	100	79.2	135.0	118.4
Open loop research based systems											
[12]	Tan, S.S.	2011	S	31.6	54	1.2	2	500	64.4	5.1	126.7
[13]a	Paavola, M.	2009	D	8.0^{E}	360	200^{C}	4	25	66.9^{C}	0.1952	112.0
[13]b	Paavola, M.	2009	S	8.0^{E}	1080	200^{C}	4	1	71.4^{C}	0.0424	109.1
[14]	Lee, W.F.	2008	D	30.0	187	1.6	2	500	55^{E}	10.0	125.2
[15]	Wu, J.F.	2004	D	35	50	1.6	6	580	74.0^{C}	30.0	124.4
[16]	Amini, B.V.	2004	D	1	12.7^{E}	200	1	75	76.2^{C}	6.0	120.6

[1] S = single die, D = dual die, C - Calculated based on numbers reported. E - Estimated

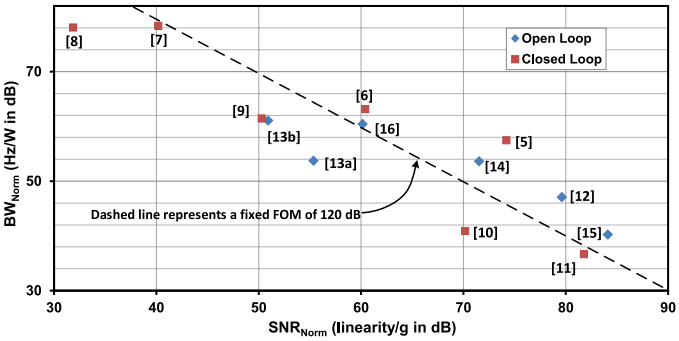

Fig. 4. Literature review in graphical form. The better performing interface circuits are at the upper right corner of the plot.

IV. Conclusion

A figure of merit for capacitive inertial sensor systems has been proposed that captures the effect of the physical specifications of the sensor on the fidelity and power consumption of the system. When normalized to the sensor's sensitivity, total sense capacitance and interface parasitic capacitance, there is a defined tradeoff between linearity and power consumption. This allows both open and closed loop systems to be easily compared with each other.

References

[1] D. Ravi *et al.*, "A deep learning approach to on-node sensor data analytics for mobile or wearable devices," *IEEE J. of Biomedical and Health Informatics*, vol. 21, pp. 56–64, January 2017.

[2] N. Yazdi *et al.*, "Precision readout circuits for capacitive microaccelerometers," in *Proceedings of IEEE Sensors, 2004.*, pp. 28–31 vol.1, Oct 2004.

[3] H. Schmid *et al.*, "A tutorial to switched-capacitor noise analysis by hand," *Analog Integrated Circuits and Signal Processing*, vol. 89, pp. 249–261, Oct 2016.

[4] W. Yun, R. T. Howe, and P. R. Gray, "Surface micromachined, digitally force-balanced accelerometer with integrated cmos detection circuitry," in *Solid-State Sensor and Actuator Workshop, 1992. 5th Technical Digest., IEEE*, pp. 126–131, June 1992.

[5] Sönmez *et al.*, "A $\Delta\Sigma$ micro accelerometer with 6 $\mu g//\sqrt{Hz}$ resolution and 130 dB dynamic range," *Analog Integrated Circuits and Signal Processing*, vol. 81, no. 2, pp. 471–485, 2014.

[6] M. Pastre *et al.*, "A 300 Hz 19b DR Capacitive Accelerometer based on a Versatile Front End in a 5^{th}-order $\Delta\Sigma$ loop," in *Proc. Eur. Solid-State Circuits Conf.*, pp. 289–292, Sept. 2009.

[7] H. Külah *et al.*, "Noise Analysis and Characterization of a Sigma-Delta Capacitive Microaccelerometer," *IEEE J. Solid-State Circuits*, vol. 41, pp. 352–360, 2006.

[8] B. V. Amini *et al.*, "A 4.5-mW Closed-Loop $\Delta\Sigma$ Micro-Gravity CMOS SOI Accelerometer," *IEEE J. Solid-State Circuits*, vol. 41, pp. 2983–2991, 2006.

[9] C. Condemine *et al.*, "A 0.8mA 50Hz 15b SNDR $\Delta\Sigma$ closed-loop 10g accelerometer using an 8^{th}-order digital compensator," in *Dig. Tech. Papers. IEEE Int. Solid-State Circuits Conf*, (San Francisco, California), pp. 248–249, Feb. 2005.

[10] V. P. Petkov and B. E. Boser, "A Fourth-Order Delta-Sigma Interface for Micromachined Inertial Sensors," *IEEE J. Solid-State Circuits*, vol. 40, pp. 1602–1609, 2005.

[11] M. Lemkin and B. E. Boser, "A Three-Axis Micromachined Accelerometer with a CMOS Position-Sense Interface and Digital Offset-Trim Electronics," *IEEE J. Solid-State Circuits*, vol. 34, pp. 456–468, 1999.

[12] S. S. Tan *et al.*, "An Integrated Low-Noise Sensing Circuit With Efficient Bias Stabilization for CMOS MEMS Capacitive Accelerometers," *IEEE Trans. Circuits Syst. I*, vol. 58, pp. 2661–2672, 2011.

[13] M. Paavola *et al.*, "A Micropower $\Delta\Sigma$-Based Interface ASIC for a Capacitive 3-Axis Micro-Accelerometer," *IEEE J. Solid-State Circuits*, vol. 44, pp. 3193–3210, 2009.

[14] W. F. Lee and P. K. Chan, "A Capacitive-Based Accelerometer IC Using Injection-Nulling Switch Technique," *IEEE Trans. Circuits Syst. I*, vol. 55, pp. 980–989, 2008.

[15] J. Wu *et al.*, "A Low-Noise Low-Offset Capacitive Sensing Amplifier for a 50 $\mu g/\sqrt{Hz}$ Monolithic CMOS MEMS Accelerometer," *IEEE J. Solid-State Circuits*, vol. 39, pp. 722–730, 2004.

[16] B. V. Amini and F. Ayazi, "A 2.5-V 14-bit $\Sigma\Delta$ CMOS SOI Capacitive Accelerometer," *IEEE J. Solid-State Circuits*, vol. 39, pp. 2467–2476, 2004.